

BinaryCoP: Binary Neural Network-based COVID-19 Face-Mask Wear and Positioning Predictor on Edge Devices

Nael Fasfous^{1*}, Manoj-Rohit Vemparala^{2*}, Alexander Frickenstein^{2*}, Lukas Frickenstein¹, Walter Stechele¹

¹ Technical University of Munich (<first_name>.<last_name>@tum.de)

² BMW Group (<first_name>.<last_name>@bmw.de)

Abstract—Face masks have long been used in many areas of everyday life to protect against the inhalation of hazardous fumes and particles. They also offer an effective solution in healthcare for bi-directional protection against air-borne diseases. Wearing and positioning the mask correctly is essential for its function. Convolutional neural networks (CNNs) offer an excellent solution for face recognition and classification of correct mask wearing and positioning. In the context of the ongoing COVID-19 pandemic, such algorithms can be used at entrances to corporate buildings, airports, shopping areas, and other indoor locations, to mitigate the spread of the virus. These application scenarios impose major challenges to the underlying compute platform. The inference hardware must be cheap, small and energy efficient, while providing sufficient memory and compute power to execute accurate CNNs at a reasonably low latency. To maintain data privacy of the public, all processing must remain on the edge-device, without any communication with cloud servers. To address these challenges, we present BinaryCoP, a low-power binary neural network classifier for correct facial-mask wear and positioning. The classification task is implemented on an embedded FPGA accelerator, performing high-throughput binary operations. Classification can take place at up to ~ 6400 frames-per-second, easily enabling multi-camera, speed-gate settings or statistics collection in crowd settings. When deployed on a single entrance or gate, the idle power consumption is reduced to 1.6W, improving the battery-life of the device. We achieve an accuracy of up to 98% for four wearing positions of the MaskedFace-Net dataset. To maintain equivalent classification accuracy for all face structures, skin-tones, hair types, and mask types, the algorithms are tested for their ability to generalize the relevant features over all subjects using the Grad-CAM approach.

I. INTRODUCTION

Convolutional neural networks (CNNs) have been applied to real-world problems since the early days of their conception [1]. In current times, the ongoing COVID-19 pandemic presents new challenges, which can be solved with the help of state-of-the-art computer vision algorithms [2], [3]. One of the most simple ways of mitigating the spread of the COVID-19 disease is wearing a face-mask, which can protect the wearer from direct exposure to the virus through the mouth and nasal passages. A correctly worn mask can also protect other people, in case the wearer is already infected with the disease. This bi-directional protection makes masks highly effective in crowded and/or indoor areas. Although face-masks have become a mandatory requirement in many public areas, it is difficult to ensure the compliance of the

general public. More specifically, it is difficult to assert that the masks are worn correctly as intended, *i.e.* completely covering the nose, mouth and chin [4].

CNNs are the current state-of-the-art in face detection applications. Compared to classical computer vision algorithms, CNNs can provide better accuracy on problems with diverse features without having to manually extract said features [5]. This holds true only when the training dataset has a fair distribution of samples. Correctly identifying a mask on a person’s face is a relatively simple task for these powerful algorithms. However, a more precise classification of the exact positioning of the mask and identifying the exposed region of the face is more challenging. To maintain equivalent classification accuracy for all face structures, skin-tones, hair types, and mask types, the algorithms must be able to generalize the relevant features over all subjects.

The deployment scenarios for the CNN should also be taken into consideration. A face-mask detector can be set at the entrance of corporate buildings, shopping areas, airport checkpoints, and speed gates. These distributed settings require cheap, battery-powered, edge devices which are limited in memory and compute power. To maintain security and data privacy of the public, all processing must remain on the edge-device without any communication with cloud servers.

Minimizing power and resource utilization while maintaining a high classification accuracy is a design challenge which necessitates hardware-software co-design. In this context, we propose Binary-CoP (Binary COVID-mask Predictor), an efficient binary neural network (BNN) classifier for real-time classification of correct face-mask wear and positioning. The challenges of the described application are tackled through the following contributions:

- Training BNNs on synthetically generated data [6] to cover a wide demographic and generalize relevant task-related features. A high accuracy of $\sim 98\%$ is achieved for a 4-class problem of mask wear and positioning.
- Deploying BNNs on a low-power, real-time embedded FPGA accelerator based on the Xilinx FINN architecture [7]. The accelerator can operate at a low-power of $\sim 1.6\text{W}$ on single entrances and gates or at high-performance (~ 6400 frames-per-second) in crowded settings.
- The BNNs are analyzed through Gradient-weighted Class Activation Mapping (Grad-CAM) to improve interpretability and study the features being learned.

* Equally contributed

II. RELATED WORK

A. COVID-19 Face-Mask Wear and Positioning

Correctly worn masks play a pivotal role in mitigating the spread of the COVID-19 disease during the ongoing pandemic [8]. Members of the general public often underestimate the importance of this simple yet effective method of disease prevention and control. Researchers and data scientists in the field of computer vision have collected data to train and deploy algorithms which help in automatically regulating masks in public spaces and indoor locations [9], [10]. Although large-scale natural face datasets exist, the number of real-world masked images is limited [9]. Wang et al. [10] extended their masked-face dataset with a Simulated Masked Face Recognition Dataset (SMFRD), which is synthetically generated by applying virtual masks to existing natural face datasets. Cabani et al. [6] improved the generation of synthetically masked-faces by applying a deformable mask-model onto natural face images with the help of automatically detected facial key-points. The key-points of the deformable mask-model can be matched to the key-points of the face, allowing the application of the mask in a variety of ways. This allows the dataset generation process to further generate examples of incorrectly worn masks, such as chin exposed, nose exposed or nose and mouth exposed.

B. Binary Neural Networks

The memory footprint of neural networks and the complexity of their arithmetic operations on inference hardware can be reduced through parameter quantization. In the most extreme case, binarizing neural networks constrains their weights and activations to $\{-1, 1\}$, such that their memory footprint is theoretically reduced by $\times 32$ compared to a float-32 CNN [11]. Additionally, simple XNOR and popcount operations can be used to implement multiply-accumulate (MAC) operations on inference hardware [12]. Specialized training schemes have been proposed to mitigate the loss in information capacity introduced by the low-bitwidth representation of BNNs [11], [13], [14], [15], [12]. In some cases, the low information capacity due to binarization can have a regularization effect which improves feature generalization [13]. This is helpful in improving the classification performance on real-world data, particularly when training on synthetically generated data [16]. In [13], Courbariaux et al. introduced a scheme to train neural networks with binary weights during forward propagation while maintaining latent full-precision values during back propagation. This ensures proper gradient flow and fine adjustments through the gradients. This approach is later extended by the binarization of activations [11]. Rastegari et al. [12] proposed XNOR-Net, where both weights and activations are binarized such that the convolutions of input feature maps and weights can be approximated by a combination of XNOR operations and popcounts, followed by a multiplication with scaling factors. The introduction of scaling factors improves the information capacity of the network at the cost of more trainable parameters for each layer. This adds to the compu-

tational complexity of XNOR-Net at deployment time. For the task of face-mask detection with low scene complexity, more efficient forms of BNNs [11] can be applied.

C. BNN Hardware Accelerators

Several accelerators have been designed to exploit the benefits of BNNs [17], [18], [7], [19], [20], [21], [22]. The Xilinx FINN [7] framework was developed to accelerate BNNs efficiently on FPGA platforms. The framework compiles high level synthesis (HLS) code from a BNN description to create a hardware design for the network. The generated streaming architecture consists of a pipeline of individual hardware components instantiated for each layer of the BNN. In this work, we deploy Binary-CoP on FINN-based hardware architectures to achieve an efficient acceleration of the masked-face inference on embedded FPGAs. We parameterize and synthesize accelerators with different hardware requirements, geared towards individual COVID-19 mask recognition (low-power) or crowd statistics collection (high-performance).

III. METHOD

This section describes the building blocks of Binary-CoP for the classification of correct mask wear and positioning.

A. Training and Inference of Binary Neural Networks

The BNN method proposed by Courbariaux et al. [11] serves as our foundation to efficiently approximate weights and activations to single bit precision at inference time, such that the neural network's arithmetic operations can be executed by simple logic operations. Smooth model training and convergence is ensured by relying on full-precision latent weights W during training time [23]. In detail, the activation tensor $A^{l-1} \in \mathbb{R}^{X_i \times Y_i \times C_i}$, with its dimensions of X_i width, Y_i height, and C_i channels, serves as the input to the convolutional layer $l \in [1, \dots, L]$. Here, A^0 and A^L represent the input image and the network's prediction, respectively. The trainable parameters of the 2D-convolutional layers are composed of the latent weight matrix $W \in \mathbb{R}^{K \times K \times C_i \times C_o}$ required for training, with kernel dimension K , input channels C_i , and output channels C_o . As previously stated, the latent weights are mapped to $\{-1, +1\}$ during the forward pass for loss calculation or deployment, resulting in the binarized $b \subset B \in \mathbb{B}^{K \times K \times C_i \times C_o}$. In the hardware implementation, -1 is expressed as a binary 0 to perform multiplications as XNOR logic operations. The $\text{sign}()$ function in Eq. 1 is used to binarize the input feature maps and weights.

$$b = \text{sign}(w) = \begin{cases} 1 & \text{if } w \geq 0, \\ -1 & \text{otherwise.} \end{cases} \quad (1)$$

The derivative of the $\text{sign}()$ function is almost always zero, resulting in insufficient gradient flow during training and back-propagation. This necessitates gradient flow approximation using a straight-through estimator (STE) [23].

Particularly for BNNs, it is of crucial importance to adjust the input elements $a^{l-1} \subset A^{l-1}$, before the approximation

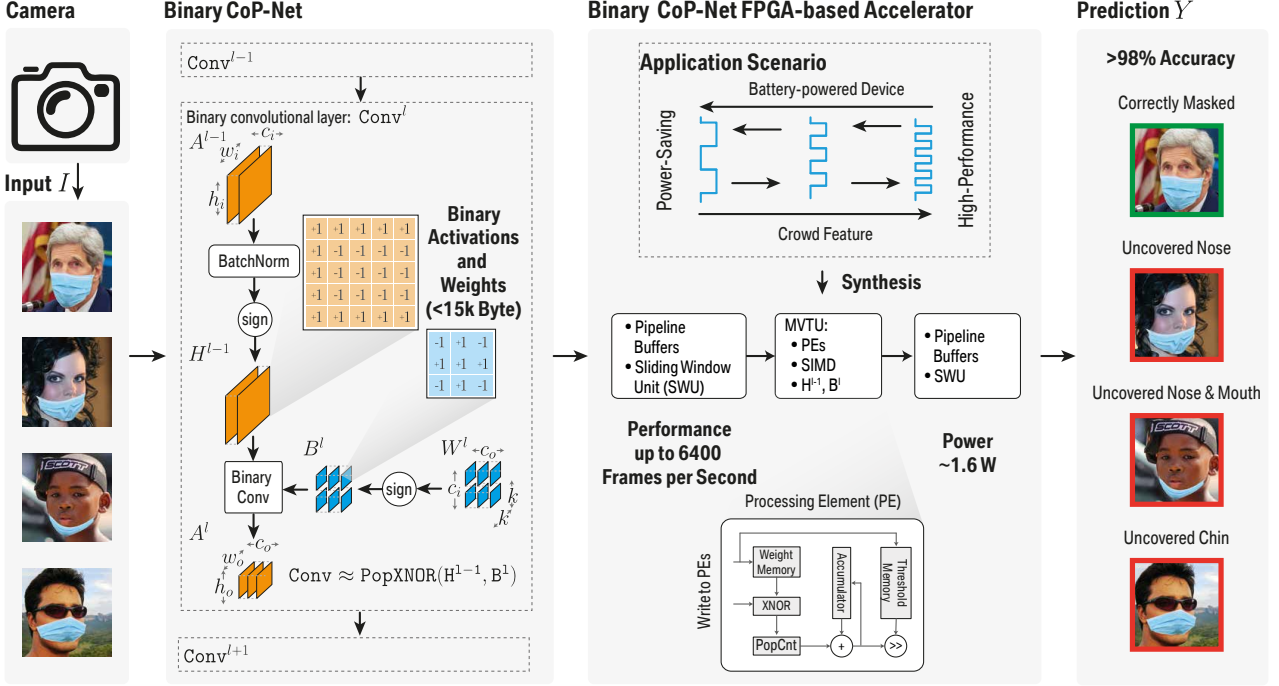


Fig. 1: Schematic representation of the Binary-CoP accelerator. A camera captures images to be classified by the neural network. The BNN accelerator is tailored for the application scenario (single gate prediction or crowd statistics collection). Binary tensors are processed in the PEs of the FPGA-based accelerator using XNOR operations. The classification of the input data is available after completion of the computations at low-latency or low-power.

into the binary representation $h^{l-1} \subset H^{l-1} \in \mathbb{B}^{X_i \times Y_i \times C_i}$ by means of batch normalization to zero mean and unit variance. An advantage of BNNs is that the result of the batch-norm operation is followed by `sign()` (see Fig. 1). Since the result after applying both functions is simply $\{-1, 1\}$, the precise calculation of the batch-norm is wasteful on embedded hardware. Based on the batch-norm statistics collected at training time, a *threshold* point τ is defined, wherein an activation value $a^{l-1} \geq \tau$ results in 1, otherwise -1 [7]. This allows the implementation of the typically costly batch-norm operation as a simple magnitude comparison operation on hardware.

Next, the binary convolution follows as:

$$H^{l-1} = \text{sign}(\text{BatchNorm}(A^{l-1})); B^l = \text{sign}(W^l) \quad (2)$$

$$A^l = \text{BinConv}(H^{l-1}, B^l) = \text{PopCnt}(\text{XNOR}(H^{l-1}, B^l)), \quad (3)$$

which results in the output feature map $A^l \in \mathbb{R}^{X_o \times Y_o \times C_o}$.

B. Hardware Architecture

The trained BNNs are conditioned for deployment on the Xilinx FINN framework [7]. The pipelined architecture offers several advantages on embedded devices, most importantly, the reduction in on-chip to off-chip memory transfers of the BNN parameters B^l and intermediate activations A^l and H^l . This is mainly feasible due to the binary format, which results in highly compact neural networks that can fit on the on-chip memory units of embedded devices. The number of processing elements (PEs), single-instruction-multiple-data (SIMD)-lanes, and other parameters can be optimized by the

designer to suit the acceleration of the trained BNN. The final design is synthesized and implemented on an embedded FPGA.

For each convolutional or fully-connected layer in the BNN, a matrix-vector-threshold unit (MVTU) is instantiated, which executes the XNOR, popcount and threshold operations mentioned in Sec. III-A. Each MVTU in the pipeline can be dimensioned for the number of PEs and SIMD lanes, which have a significant impact on hardware resource utilization, latency and the effective throughput of the pipeline. Based on the compute complexity of each layer, the available hardware resources need to be distributed over the corresponding MVTUs, such that all parts of the pipeline have a matched-throughput. A single under-dimensioned MVTU could throttle the entire pipeline, resulting in sub-optimal throughput. A single MVTU of the pipeline is shown in Fig. 1, and a corresponding PE is detailed.

For convolutional layers, an additional sliding-window unit (SWU) reshapes the binarized activation maps to create a single, wide input feature map memory, which can efficiently be accessed by the corresponding MVTU. Max-pool layers are implemented as boolean OR operations, since a single binary “1” value suffices to make the entire pool window output equal to 1.

C. BNN Interpretability with Grad-CAM

The output of the convolutional layers in a CNN contains localized information of the input image, without any prior bias on the location of objects and features during training. This information can be captured using Class Activation

Mapping (CAM) [24] and Gradient-weighted Class Activation Mapping (Grad-CAM) [25] techniques. To apply CAM, the model must end with a global average pooling layer followed by a fully-connected layer, providing the logits of a particular input. The BNN models investigated in this work operate on a small input resolution of 32×32 , and achieve a high reduction of spatial information without incorporating a global average pooling layer. For this reason, the Grad-CAM approach is better-suited to obtain visual interpretations of Binary-CoP's attention and determine the important regions for its predictions of different inputs and classes.

To obtain the class-discriminative localization map, we consider the activations and gradients for the output of the `conv2_2` layer, which has spatial dimensions of 5×5 . We use average pooling for the corresponding gradients and reduce the channels by performing Einstein summation as specified in [25]. With this approach the base networks do not need any modifications or retraining. Due to the synthetically generated dataset used for training, we expect Binary-CoP models to generalize well against domain shifts.

IV. RESULTS AND DESIGN SPACE EXPLORATION

A. Experimental Setup

Binary-CoP is able to detect the presence of a mask, as well as its position and correctness. This level of classification detail is possible through the more detailed split of the MaskedFace-Net dataset [6] from 2 classes, namely Correctly Masked Face Dataset (CMFD) and Incorrectly Masked Face Dataset (IMFD), to 4 classes of CMFD, IMFD Nose, IMFD Chin, and IMFD Nose and Mouth. The dataset suffers from high imbalance in the number of samples per class. From the total 133,783 samples, roughly 5% of the samples are IMFD Chin, and another 5% samples are IMFD Nose and Mouth. CMFD samples make up 51% of the total dataset while IMFD Nose makes up 39%. The dataset in its raw distribution would heavily bias the training towards the two dominant classes. To counter this, we randomly sample the larger classes CMFD and IMFD Nose to collect a comparable number of examples to the two remaining classes, IMFD Chin and IMFD Nose and Mouth. The evenly balanced dataset is then randomly augmented with a varying combination of contrast, brightness, gaussian noise, flip and rotate operations. The final size of the balanced dataset is 110K train and validation examples and 28K test samples. The images are resized to 32×32 pixels, similar to the CIFAR-10 [26] dataset. The BNNs are trained up to 300 epochs, unless learning saturates earlier. The full-precision (FP32) variant used for the Grad-CAM comparison is trained for 175 epochs due to early learning saturation (98.6% final test accuracy). We trained the BNN architectures shown in Tab. I according to the method described in Sec.III-A. Each convolutional (Conv) and fully connected (FC) layer is followed by batch-norm and activation layers except for the final layer. Conv groups 1 and 2 are followed by a max-pool layer. The target System-on-Chip (SoC) platform for the experiments is the Xilinx XC7Z020 (Z7020) chip. The μ -CNV design can also be synthesized for the more constrained

XC7Z010 (Z7010) chip, when XNOR operations are offloaded to the DSP blocks as described in [27]. Power and throughput measurements are taken directly on a running system. The power is measured at the power supply of the board (includes both PS and PL). The throughput reported is the classification rate when the accelerator's pipeline is full.

TABLE I: Network architectures and hardware dimensioning.

Network	CNV	n -CNV	μ -CNV
Arch.	Conv _{1,1} [3, 64] Conv _{1,2} [64, 64] Conv _{2,1} [64, 128] Conv _{2,2} [128, 128] Conv _{3,1} [128, 256] Conv _{3,2} [256, 256] FC ₁ [512] FC ₂ [512] FC ₃ [4]	Conv _{1,1} [3, 16] Conv _{1,2} [16, 16] Conv _{2,1} [16, 32] Conv _{2,2} [32, 32] Conv _{3,1} [32, 64] Conv _{3,2} [64, 64] FC ₁ [128] FC ₂ [128] FC ₃ [4]	Conv _{1,1} [3, 16] Conv _{1,2} [16, 16] Conv _{2,1} [16, 32] Conv _{2,2} [32, 32] Conv _{3,1} [32, 64] FC ₁ [128] FC ₂ [4]
PE Count	16, 32, 16, 16, 4, 1, 1, 1, 4	16, 16, 16, 16, 4, 1, 1, 1, 1	4, 4, 4, 4, 1, 1, 1
SIMD lanes	3, 32, 32, 32, 32, 32, 4, 8, 1	3, 16, 16, 32, 32, 32, 4, 8, 1	3, 16, 16, 32, 32, 16, 1

B. Design Space Exploration

We evaluate three Binary-CoP prototypes, namely CNV, n -CNV and μ -CNV. The CNV network is based on the architecture in [7] inspired by VGG-16 [28] and BinaryNet [11]. n -CNV is a downsized version for a smaller memory footprint, and μ -CNV has fewer layers to reduce the size of the synthesized design. All designs are synthesized with a target clock frequency of 100MHz.

In Tab. II, the hardware utilization for the Binary-CoP prototypes is provided. With μ -CNV, a significant reduction in LUTs is achieved, which makes the design synthesizable on the heavily constrained Z7010 SoC. The trade-off is a slight increase in the memory footprint of the BNN, as the shallower network has a larger spatial dimension before the fully-connected layers, increasing the total number of parameters after the last convolutional layer. The choice of PE count and SIMD lanes for the n -CNV prototype allow it to reach a maximum throughput of ~ 6400 classifications per second when its pipeline is full. This high-performance can be used to split large crowd images and classify them at a high-rate to detect uncovered faces in a scene. Conversely, for single entrance/gate classifications, all prototypes have an idle power of around 1.6W, which is required mostly by the soft-core on the SoC. In this setting, a classification needs to be triggered only when a subject is attempting to pass through the entrance where Binary-CoP is deployed.

C. Grad-CAM Analysis

The confusion matrix in Fig. 2 shows the generalization of Binary-CoP-CNV on all classes after balancing the dataset. We further analyze the output heat maps generated by Grad-CAM to interpret the predictions of our BNNs with respect to the diverse attributes of the MaskedFace-Net dataset. In Fig. 3 - Fig. 9, column 1 and 2 indicate the label and input image respectively. Columns 3, 4 and 5 highlight the heat maps obtained from the Grad-CAM output of Binary-CoP-CNV, Binary-CoP- n -CNV and a full-precision version of CNV with float-32 parameters (FP32). The heat maps are overlaid on the raw input images for better visualization. All raw images chosen have been classified correctly by all

TABLE II: Hardware results of design space exploration.

Configuration	LUT	BRAM	DSP	Acc.
CNV	26060	124	24	98.10
<i>n</i> -CNV	20425	10.5	14	93.94
μ -CNV	11738	14	27	93.78

		True Class			
		Correct	Nose	N+M	Chin
Predicted Class	Correct	7125 98%	41 1%	1 0%	90 1%
	Nose	26 0%	7042 98%	94 2%	26 0%
True Class	N+M	4 0%	79 1%	5651 98%	9 0%
	Chin	107 1%	41 1%	7 0%	7363 98%

Fig. 2: Confusion matrix of Binary-CoP-CNV on the test set.

the networks, for fair interpretation of feature-to-prediction correlation.

In Fig. 3, we analyze the Region of Interest (RoI) for the correctly masked class. Binary-CoP’s learning capacity allows it to focus on key facial lineaments of the human wearing the mask, rather than the mask itself. This potentially helps in generalizing on other mask types. For the child example shown in the first row, the focus of Binary-CoP variants lies on the nose, making sure that it is fully covered by the mask. Similarly, for the adult in row 2, Binary-CoP-CNV focuses on the exposed cheekbones, to assert its correct mask prediction. This also holds for our small version of Binary-CoP, with significantly reduced learning capacity. The RoI curves finely above the mask, tracing the exposed region of the face. In the third row example, Binary-CoP-CNV falls back to focusing on the mask, whereas Binary-

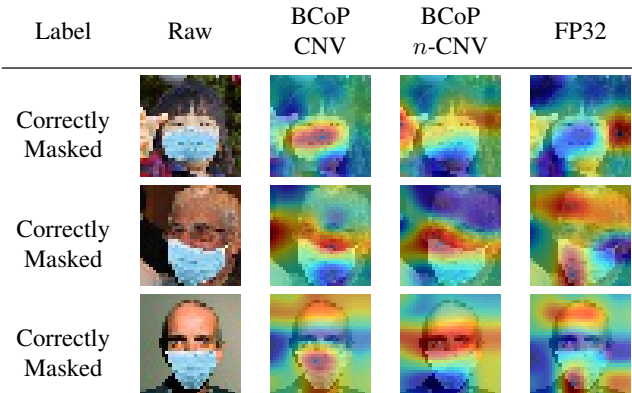


Fig. 3: Grad-CAM results for the correctly-masked class.

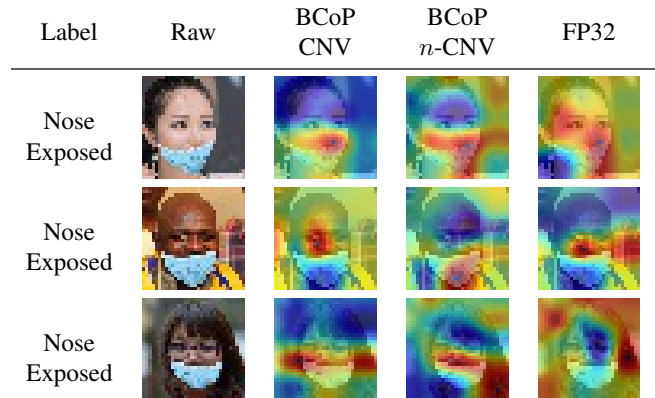


Fig. 4: Grad-CAM results for the nose-exposed class.

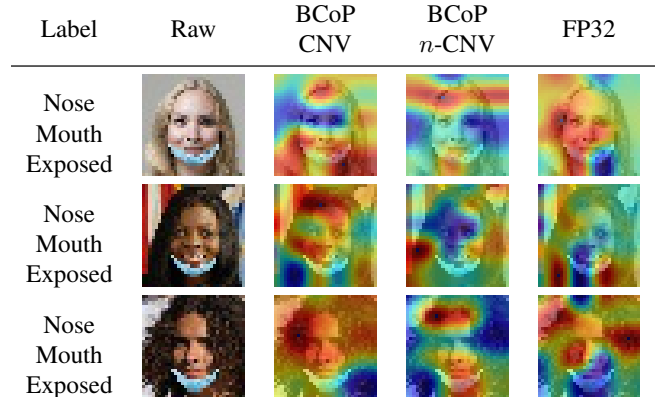


Fig. 5: Grad-CAM results for the nose and mouth-exposed class.

CoP-*n*-CNV continues to focus on the exposed features. Both models achieve the same prediction by focusing on different parts of the raw image. In contrast to the Binary-CoP variants, the full precision FP32 model seems to focus on a combination of several different features. This can be attributed to its larger learning capacity.

In Fig. 4, we analyze the Grad-CAM output of the uncovered nose class. Binary-CoP-CNV and Binary-CoP-*n*-CNV focus specifically on two regions, namely the nose and the straight upper edge of the mask. These clear characteristics cannot be observed with the oversized FP32 CNN. In Fig 5, the results show the RoI for predicting the exposed mouth and nose class. All models seem to distribute their attention onto several exposed features of the face.

Fig. 6 shows Grad-CAM results which predict the chin being exposed. The top region of the mask points upwards, similar to the correctly worn mask. Therefore, the BNNs pay less attention to this region and instead focus on the neck and chin. With the full precision FP32 model, it is difficult to interpret the reason for the correct classification, as little to no focus is given to the chin region.

Beyond studying the BNNs’ behavior on different class predictions, we can use the attention heat maps to understand the generalization behavior of the classifier. In Fig. 7 - Fig. 9,

Label	Raw	BCoP CNV	BCoP n -CNV	FP32
Chin Exposed				
Chin Exposed				
Chin Exposed				

Fig. 6: Grad-CAM results for the chin-exposed class.

Label	Raw	BCoP CNV	BCoP n -CNV	FP32
Correctly Masked				
Correctly Masked				
Correctly Masked				

Fig. 7: Grad-CAM results for age generalization.

we test Binary-CoP’s generalization over ages, hair colors and head gear, as well as complete face manipulation with double-masks, face paint and sunglasses. In Fig 7, we see that the smaller eyes of infants and elderly do not hinder Binary-CoP’s ability to focus on the top region of the correctly worn masks. In Fig. 8, Binary-CoP-CNV shows resilience to differently colored hair and head-gear, even when having a similar light-blue color as the face-masks (row 2 and 3). In contrast, the FP32 model’s attention seems to shift towards the hair and head-gear for these cases. Finally, in Fig. 9, both Binary-CoP variants focus on relevant features of the corresponding label, irrespective of the obscured or manipulated faces. This empirically shows that the complex training of BNNs, along with their lower information capacity, constrains them to focus on a smaller set of relevant features, thereby generalizing well for unprecedented cases.

V. CONCLUSION

In this paper, we apply binary neural networks to the task of classifying the correctness of face-mask wear and positioning. In the context of the ongoing COVID-19 pandemic, such algorithms can be used at entrances to corporate buildings, airports, shopping areas, and other indoor locations to mitigate the spread of the virus. Applying BNNs to this application solves several challenges such as (1) Maintaining data privacy of the public by processing data on the edge-

Label	Raw	BCoP CNV	BCoP n -CNV	FP32
Correctly Masked				
Correctly Masked				
Nose Exposed				

Fig. 8: Grad-CAM results for hair/headgear generalization.

Label	Raw	BCoP CNV	BCoP n -CNV	FP32
Correctly Masked				
Correctly Masked				
Chin Exposed				
Nose Mouth Exposed				
Nose Mouth Exposed				

Fig. 9: Grad-CAM results for face manipulation with double-masks, face paint and sunglasses.

device, (2) Deploying the classifier on an efficient XNOR-based accelerator to achieve low-power computation, and (3) Minimizing the neural network’s memory footprint by representing all parameters in the binary domain, enabling deployment on low-cost, embedded hardware. The accelerator requires only $\sim 1.6\text{W}$ of power for operation on single gates/entrances. Alternatively, high-performance is possible, providing fast batch classification for statistics collection in crowded settings at ~ 6400 frames-per-second. We achieve an accuracy of up to 98% for four wearing positions of the MaskedFace-Net dataset. The Grad-CAM approach is used to study the features learned by the proposed Binary-CoP classifier. The results show the classifier’s high generalization ability, allowing it to perform well on different face structures, skin-tones, hair types, and age groups.

REFERENCES

- [1] Y. Lecun, L. Bottou, Y. Bengio, and P. Haffner, “Gradient-based learning applied to document recognition,” *Proceedings of the IEEE*,

vol. 86, no. 11, pp. 2278–2324, 1998.

[2] L. Wang and A. Wong, “Covid-net: A tailored deep convolutional neural network design for detection of covid-19 cases from chest x-ray images,” 2020.

[3] A. I. Khan, J. L. Shah, and M. M. Bhat, “Coronet: A deep neural network for detection and diagnosis of covid-19 from chest x-ray images,” *Computer Methods and Programs in Biomedicine*, vol. 196, p. 105581, Nov 2020. [Online]. Available: <http://dx.doi.org/10.1016/j.cmpb.2020.105581>

[4] “When and how to use masks.” [Online]. Available: <https://www.who.int/emergencies/diseases/novel-coronavirus-2019/advice-for-public/when-and-how-to-use-masks>

[5] N. O’Mahony, S. Campbell, A. Carvalho, S. Harapanahalli, G. V. Hernandez, L. Krpalkova, D. Riordan, and J. Walsh, “Deep learning vs. traditional computer vision,” in *Advances in Computer Vision*, K. Arai and S. Kapoor, Eds. Cham: Springer International Publishing, 2020, pp. 128–144.

[6] A. Cabani, K. Hammoudi, H. Benhabiles, and M. Melkemi, “Maskedface-net – a dataset of correctly/incorrectly masked face images in the context of covid-19,” *Smart Health*, 2020. [Online]. Available: <http://www.sciencedirect.com/science/article/pii/S2352648320300362>

[7] Y. Umuroglu, N. J. Fraser, G. Gambardella, M. Blott, P. Leong, M. Jahre, and K. Vissers, “Finn: A framework for fast, scalable binarized neural network inference,” in *Proceedings of the 2017 ACM/SIGDA International Symposium on Field-Programmable Gate Arrays*, ser. FPGA ’17. New York, NY, USA: ACM, 2017, pp. 65–74. [Online]. Available: <http://doi.acm.org/10.1145/3020078.3021744>

[8] T. Mitze, R. Kosfeld, J. Rode, and K. Wälde, “Face masks considerably reduce covid-19 cases in germany,” *Proceedings of the National Academy of Sciences*, vol. 117, no. 51, pp. 32 293–32 301, 2020. [Online]. Available: <https://www.pnas.org/content/117/51/32293>

[9] S. Ge, J. Li, Q. Ye, and Z. Luo, “Detecting masked faces in the wild with lle-cnns,” in *2017 IEEE Conference on Computer Vision and Pattern Recognition (CVPR)*, 2017, pp. 426–434.

[10] Z. Wang, G. Wang, B. Huang, Z. Xiong, Q. Hong, H. Wu, P. Yi, K. Jiang, N. Wang, Y. Pei, H. Chen, Y. Miao, Z. Huang, and J. Liang, “Masked face recognition dataset and application,” 2020.

[11] I. Hubara, M. Courbariaux, D. Soudry, R. El-Yaniv, and Y. Bengio, “Binarized neural networks,” in *Advances in Neural Information Processing Systems 29*. Curran Associates, Inc., 2016, pp. 4107–4115. [Online]. Available: <http://papers.nips.cc/paper/6573-binarized-neural-networks.pdf>

[12] M. Rastegari, V. Ordonez, J. Redmon, and A. Farhadi, “XNOR-Net: ImageNet Classification Using Binary Convolutional Neural Networks,” in *The European Conference on Computer Vision (ECCV)*. Cham: Springer International Publishing, 2016, pp. 525–542.

[13] M. Courbariaux, Y. Bengio, and J.-P. David, “Binaryconnect: Training deep neural networks with binary weights during propagations,” in *Advances in Neural Information Processing Systems (NeurIPS)*, C. Cortes, N. D. Lawrence, D. D. Lee, M. Sugiyama, and R. Garnett, Eds. Curran Associates, Inc., 2015, pp. 3123–3131.

[14] S. Darabi, M. Belbahri, M. Courbariaux, and V. P. Nia, “BNN+: improved binary network training,” *CoRR*, vol. abs/1812.11800, 2018. [Online]. Available: <http://arxiv.org/abs/1812.11800>

[15] X. Lin, C. Zhao, and W. Pan, “Towards accurate binary convolutional neural network,” in *Advances in Neural Information Processing Systems 30*, I. Guyon, U. V. Luxburg, S. Bengio, H. Wallach, R. Fergus, S. Vishwanathan, and R. Garnett, Eds. Curran Associates, Inc., 2017, pp. 345–353. [Online]. Available: <http://papers.nips.cc/paper/6638-towards-accurate-binary-convolutional-neural-network.pdf>

[16] A. Frickenstein, M.-R. Vemparala, J. Mayr, N.-S. Nagaraja, C. Unger, F. Tombari, and W. Stechele, “Binary DAD-Net: Binarized Drivable Area Detection Network for Autonomous Driving,” in *International Conference on Robotics and Automation (ICRA)*, Paris, France, 2020.

[17] R. Andri, L. Cavigelli, D. Rossi, and L. Benini, “Yodann: An architecture for ultralow power binary-weight cnn acceleration,” *IEEE Transactions on Computer-Aided Design of Integrated Circuits and Systems*, vol. 37, no. 1, pp. 48–60, Jan 2018.

[18] K. Ando, K. Ueyoshi, K. Orimo, H. Yonekawa, S. Sato, H. Nakahara, S. Takamaeda-Yamazaki, M. Ikebe, T. Asai, T. Kuroda, and M. Motomura, “Brein memory: A single-chip binary/ternary reconfigurable in-memory deep neural network accelerator achieving 1.4 tops at 0.6 w,” *IEEE Journal of Solid-State Circuits*, vol. 53, no. 4, pp. 983–994, April 2018.

[19] S. Liang, S. Yin, L. Liu, W. Luk, and S. Wei, “Fp-bnn,” *Neurocomput.*, vol. 275, no. C, p. 1072–1086, Jan. 2018. [Online]. Available: <https://doi.org/10.1016/j.neucom.2017.09.046>

[20] P. Guo, H. Ma, R. Chen, P. Li, S. Xie, and D. Wang, “Fbna: A fully binarized neural network accelerator,” in *2018 28th International Conference on Field Programmable Logic and Applications (FPL)*, 2018, pp. 51–513.

[21] E. Nurvitadhi, D. Sheffield, Jaewoong Sim, A. Mishra, G. Venkatesh, and D. Marr, “Accelerating binarized neural networks: Comparison of fpga, cpu, gpu, and asic,” in *2016 International Conference on Field-Programmable Technology (FPT)*, 2016, pp. 77–84.

[22] C. Fu, S. Zhu, H. Su, C.-E. Lee, and J. Zhao, “Towards fast and energy-efficient binarized neural network inference on fpga,” in *Proceedings of the 2019 ACM/SIGDA International Symposium on Field-Programmable Gate Arrays*, ser. FPGA ’19. New York, NY, USA: Association for Computing Machinery, 2019, p. 306. [Online]. Available: <https://doi.org/10.1145/3289602.3293990>

[23] Y. Bengio, N. Léonard, and A. C. Courville, “Estimating or propagating gradients through stochastic neurons for conditional computation,” *CoRR*, vol. abs/1308.3432, 2013. [Online]. Available: <http://arxiv.org/abs/1308.3432>

[24] B. Zhou, A. Khosla, A. Lapedriza, A. Oliva, and A. Torralba, “Learning deep features for discriminative localization,” in *IEEE/CVF Conference on Computer Vision and Pattern Recognition (CVPR)*, June 2016, pp. 2921–2929.

[25] R. R. Selvaraju, M. Cogswell, A. Das, R. Vedantam, D. Parikh, and D. Batra, “Grad-cam: Visual explanations from deep networks via gradient-based localization,” in *Proceedings of the IEEE International Conference on Computer Vision (ICCV)*, Oct 2017.

[26] A. Krizhevsky, “Learning multiple layers of features from tiny images,” *University of Toronto*, 2009.

[27] N. Fasfous, M. R. Vemparala, A. Frickenstein, and W. Stechele, “Or-thruspe: Runtime reconfigurable processing elements for binary neural networks,” in *2020 Design, Automation Test in Europe Conference Exhibition (DATE)*, 2020, pp. 1662–1667.

[28] K. Simonyan and A. Zisserman, “Very deep convolutional networks for large-scale image recognition,” in *International Conference on Learning Representations*, 2015.